Pharm Res (2013) 30:792–802
DOI 10.1007/s11095-012-0920-4

RESEARCH PAPER

Skin Permeation of Small-Molecule Drugs, Macromolecules, and Nanoparticles Mediated by a Fractional Carbon Dioxide Laser: The Role of Hair Follicles

Woan-Ruoh Lee • Shing-Chuan Shen • Saleh A. Al-Suwayeh • Hung-Hsu Yang • Yi-Ching Li • Jia-You Fang

Received: 24 June 2012 / Accepted: 18 October 2012 / Published online: 10 November 2012

ABSTRACT

Purpose To evaluate skin permeation enhancement mediated by fractional laser for different permeants, including hydroquinone, imiquimod, fluorescein isothiocyanate-labeled dextran (FD), and quantum dots.

Methods Skin received a single irradiation of a fractional CO_2 laser, using fluence of 2 or 4 mJ with densities of 100~400 spots/cm^2. *In vitro* and *in vivo* skin penetration experiments were performed. Fluorescence and confocal microscopies for imaging delivery pathways were used.

Results The laser enhanced flux of small-molecule drugs 2~5-fold compared to intact skin. A laser fluence of 4 mJ with a 400-spot/cm^2 density promoted FD flux at 20 and 40 kDa from 0 (passive transport) to 0.72 and 0.43 nmol/cm^2/h, respectively. Microscopic images demonstrated a significant increase in fluorescence accumulation and penetration depth of macromolecules and nanoparticles after laser exposure. Predominant routes for laser-assisted delivery may be intercellular and follicular transport. CO_2 laser irradiation produced 13-fold enhancement in follicular deposition of imiquimod. Laser-mediated follicular transport could deliver permeants to deeper strata. Skin barrier function as determined by transepidermal water loss completely recovered by 12 h after irradiation, much faster than conventional laser treatment (4 days).

Conclusions Fractional laser could selectively enhance permeant targeting to follicles such as imiquimod and FD but not hydroquinone, indicating the importance of selecting feasible drugs for laser-assisted follicle delivery.

KEY WORDS fractional CO_2 laser · hair follicles · macromolecule · nanoparticle · skin permeation · small-molecule drug

INTRODUCTION

Skin delivery systems are used for topical and transdermal purposes. They are both user-friendly and painless which help increase patient compliance. However, only a few drugs are candidates for skin delivery due to the barrier function of the stratum corneum (SC) (1). Several chemical and physical techniques were investigated to enhance skin permeability. Among these, laser treatment is a noteworthy trend. A resurfacing laser can precisely ablate the SC layers in a controlled manner by adjusting the laser parameters (2). The duration of laser irradiation is only nano- or microseconds, suggesting enhancement of skin permeation in very short treatment times (3). Furthermore, laser irradiates the skin in a non-contact fashion which avoids cross-contamination risks. The laser energy for increasing drug skin delivery is consistently lower than that for treating wrinkles, scarring, and photodamage (4), assuring its better safety toward the skin.

The carbon dioxide (CO_2) laser is a resurfacing laser which can remove the SC, thus enhancing drug delivery via the skin. SC ablation by a CO_2 laser is accompanied by undesirable residual thermal effects. The heating procedure

W.-R. Lee • S.-C. Shen • H.-H. Yang
Graduate Institute of Medical Sciences, Taipei Medical University
Taipei 110, Taiwan

W.-R. Lee
Department of Dermatology
Taipei Medical University—Shuang Ho Hospital
Taipei 235, Taiwan

S. A. Al-Suwayeh
Department of Pharmaceutics, College of Pharmacy
King Saud University
Riyadh, Saudi Arabia

Y.-C. Li • J.-Y. Fang (✉)
Pharmaceutics Laboratory, Graduate Institute of Natural Products
Chang Gung University
259 Wen-Hwa 1st Road
Kweishan, Taoyuan 333, Taiwan
e-mail: fajy@mail.cgu.edu.tw

can result in loss of cell function and tissue necrosis (5). Our previous study demonstrated that a 4-day duration was needed to recover the SC barrier function after CO_2 laser treatment, although this laser greatly enhanced 5-fluorouracil absorption (6). This drawback may limit the applicability of CO_2 lasers. Fractional lasers recently became popular as they only treat a portion of the irradiated skin. They use microscopic areas of illumination surrounded by islands of normal tissues (7). The fractional technology offers significant advantages of a safe procedure which permits rapid reepithelialization. In 2007, this concept was introduced for CO_2 lasers (8,9). The fractional CO_2 laser may resolve the problems of the long wound-healing duration of conventional lasers. In the present work, we evaluated the pretreatment effect of a fractional laser on the skin permeation of small-molecule drugs, macromolecules, and nanoparticles. We tried to set specific laser conditions for optimal treatment recommendations. Since appendageal routes are essential for the permeation of certain drugs, especially macromolecules, the second aim was to explore the role of hair follicles in skin delivery enhanced by a fractional laser.

Hydroquinone and imiquimod were selected as the model drugs as small-molecule permeants. Hydroquinone is a hydrophilic drug used to treat hyperpigmentation disorders (10). Imiquimod is a lipophilic drug used to manage warts, skin carcinomas, and skin aging (11). Macromolecules such as proteins, nucleotides, and small interfering (si)RNA are currently being investigated for topical therapy (12). Suitable enhancing methods are necessary to improve the skin transport of macromolecules since it is impossible for them to passively permeate the SC. To test the feasibility of laser enhancement, fluorescein isothiocyanate (FITC)-labeled dextran (FD) of various molecular weights (MWs) was used as the macromolecular model. The skin absorption of nanocrystal quantum dots (QDs) with a diameter of 18 nm was also examined in this study. Both *in vitro* and *in vivo* skin permeation experiments were carried out using nude mouse as an animal model. The distribution of permeants in the skin was imaged by fluorescence microscopy and confocal laser scanning microscopy (CLSM). Recovery of the skin barrier function post-irradiation was detected by the transepidermal water loss (TEWL).

J.-Y. Fang
Department of Cosmetic Science
Chang Gung University of Science and Technology
Kweishan, Taoyuan, Taiwan

Y.-C. Li
Chinese Herbal Medicine Research Team, Healthy Aging Research Center
Chang Gung University
Kweishan, Taoyuan, Taiwan

MATERIALS AND METHODS

Materials

Hydroquinone, FITC, and FD with average MWs of 4 (FD4), 10 (FD10), 20 (FD20), and 40 kDa (FD40) were purchased from Sigma-Aldrich (St. Louis, MO, USA). Imiquimod was supplied by LKT Laboratories (St. Paul, MN, USA). The carboxylic acid-conjugated QDs (Qdot® 800 ITK) were provided by Invitrogen (Carlsbad, CA, USA).

Fractional CO_2 Laser

The fractional laser with a wavelength of 10,600 nm and pulse times of 60 and 80 μs for 2 and 4 mJ was purchased from Lutronic (eCO_2®, San Jose, CA, USA). The handpiece creates microscopic columns of skin ablation, which are called microscopic treatment zones (MTZs). The MTZs used in this study were 120 and 300 μm in diameter. The scan area size was 1.2×1.2 cm. The spot numbers in this area were set to 100, 200, or 400 spots/cm^2. The MTZ coverage extents in the area treated by a 120-μm MTZ would be 1.8%, 3.7%, and 7.3% for 100, 200, and 400 spots/cm^2, respectively. Laser fluences of 2 and 4 mJ were used to irradiate nude mouse skin.

Animals

Female nude mice (ICR-Foxn1nu strain) aged 8 weeks were obtained from the National Laboratory Animal Center (Taipei, Taiwan). The animal experimental protocol was reviewed and approved by the Institutional Animal Care and Use Committee of Chang Gung University.

Histological Examination of the Skin

The laser was used to irradiate the dorsal region of nude mice. The animals were sacrificed, and specimens of the laser-treated area were excised. Each skin sample was fixed in 10% buffered formaldehyde using ethanol, embedded in paraffin wax, and stained with hematoxylin and eosin (H&E). Cyclooxygenase (COX)-2 immunostaining was performed based on our previous study (13). Biopsies were examined and imaged under light microscopy (IX81, Olympus, Tokyo, Japan).

In Vitro Skin Permeation

This experiment was conducted with Franz diffusion cells. The full-thickness skin of a nude mouse was taken from the dorsal region. The skin was treated with a fractional CO_2 laser and then mounted between the donor and receptor compartments of a Franz cell with the SC facing upwards

into the donor compartment. A pH 7.4 phosphate buffer (5.5 ml) was used as the receptor medium for hydroquinone, FITC, and FD. The medium for imiquimod was 20% ethanol in pH 7.4 buffer. The donor was pipetted with 0.5 ml of hydroquinone in pH 7 buffer (0.11%, *w/v*), imiquimod in 20% ethanol/pH7.4 buffer (0.1%), FITC/FD in double-distilled water (120 μM), or QDs in pH 7.4 buffer (0.8 μM). The permeation area between compartments was 0.785 cm^2. The stirring rate was maintained at 600 rpm and the temperature at 37°C. A 300-μl aliquot was withdrawn from the receptor at determined intervals, and was immediately replaced with an equal volume of fresh medium. Samples of hydroquinone and imiquimod were analyzed by high-performance liquid chromatography (HPLC) as described previously (14,15). The receptor accumulation amounts of FITC and FD were quantified by a fluorescence spectrophotometer (F-2500, Hitachi, Tokyo, Japan). The amount of selenium from the QDs was analyzed with an atomic absorption spectrophotometer (Z-5000, Hitachi).

Differential Stripping and Cyanoacrylate Skin Surface Biopsy

This method was utilized to examine the amount of small-molecule drugs in hair follicles (16). After a 24-h application, the skin was removed from the Franz cell and the SC was stripped by applying adhesive tape 20 times. Subsequent to tape stripping, follicular casts were prepared. A drop of superglue (ethyl cyanoacrylate 7004T, 3M, Taipei, Taiwan) was positioned on a glass slide, which was then pressed onto the surface of the stripped skin. The cyanoacrylate was polymerized, and the slide was removed with one quick movement after 5 min. The superglue remaining on the slide was scrapped off, and then positioned in a test tube containing 2 ml methanol. The tube was shaken for 3 h. The resulting mixture was vacuumed to evaporate the methanol. The mobile phase was added to the sample for the HPLC analysis.

Fluorescence Microscopy

Immediately after *in vitro* skin permeation application, specimens of the permeated skin area were used for monitoring by fluorescence microscopy. The skin biopsies were cut vertically, embedded in OCT, and frozen at −70°C. Samples were subsequently sectioned in a cryostat microtome and mounted with glycerin and gelatin. The slices were examined with an inverted microscope (IX81, Olympus) using a filter set at 450~490 and 515~565 nm for excitation and emission, respectively. The excitation and emission wavelengths for QDs were 546 and 590 nm, respectively.

In Vivo Skin Permeation

A mouse's back was irradiated with a fractional laser. Subsequently, a glass cylinder with an available area of 0.785 cm^2 was fixed onto the treated skin with glue. The cylinder was filled with double-distilled water containing 120 μM FITC or FD20 (0.2 ml). The application time for the permeants was 2 h. The animal was sacrificed, and the skin was excised to examine the fluorescence signal by confocal laser scanning microscopy (CLSM). The skin surface was washed with methanol to remove residual permeants. The skin thickness was optically scanned at 5-μm increments through the Z-axis of a Leica TCS SP2 confocal microscope (Wetzlar, Germany). Optical excitation and emission wavelengths were set to 488 and 500~535 nm, respectively.

Recovery of the Skin Barrier Function

The dorsal skin of a nude mouse was treated with the fractional laser at 2 or 4 mJ. Transepidermal water loss (TEWL) values were measured by a Tewameter (TM300, Courage and Khazaka, Köln, Germany) for 24 h post-irradiation. The baseline standard was determined using adjacent untreated skin. The temperature and relative humidity in the laboratory were kept at 25°C and 55%, respectively.

Statistical Analysis

The analysis was carried out using an unpaired Student's *t*-test or analysis of variance (ANOVA). A 0.05 level of probability ($p<0.05$) was accepted as statistically significant.

RESULTS

Histological Examination of Skin

Biopsy specimens of laser-treated skin were obtained immediately after irradiation for a blinded histological assay as shown in Fig. 1. For this experiment, the MTZ was fixed at 120 μm, and the fluence was set to 2 or 4 mJ. As shown in Fig. 1a, light microscopy indicated no observable damage to the entire skin in the non-treated group. Irradiation with 2 mJ showed partial removal of the SC with no disruption of the epidermis or dermis (Fig. 1b). Fractional laser treatment at 4 mJ led to the formation of cone-shaped pores with depths ranging 25~30 μm (arrow in Fig. 1c). Some SC layers still remained at the top of the pore after treatment. A 4-mJ pulse resulted in partial epidermal ablation and epidermal necrosis and coagulation. An intact morphology

of the dermis was found under the irradiated site. For the fluence at 4 mJ, infiltrating inflammatory cells were observed. This is in marked contrast to the lower fluence (2 mJ) for which no infiltration was detected. There was no observable change in the morphology surrounding the MTZs. COX-2 expression in the untreated skin is shown in Fig. 1d. COX-2 was predominantly located in the epidermis. The laser fluence of 2 mJ produced comparable expression to that of the control group (Fig. 1e). On the other hand, the laser at 4 mJ induced higher COX-2 expression in the treated area than that at the lower fluence (arrow in Fig. 1f).

In Vitro Skin Permeation

Hydroquinone was first selected to examine the feasibility of laser-assisted skin delivery. *In vitro* skin permeation was studied by varying the fluences and numbers of pores. Both MTZs of 120 and 300 μm were irradiated for comparison. Figure 2a illustrates hydroquinone accumulation in receptors with an MTZ of 120 μm. All tested fluences were effective in increasing hydroquinone permeation. A higher fluence (4 mJ) increased hydroquinone permeation to a greater level ($p<0.05$) compared to the lower fluence (2 mJ). An increase in spot numbers in a fixed area generally increased hydroquinone delivery. Nevertheless, there was no significant difference ($p>0.05$) between permeation at 200 and 400 spots/cm^2. The drug permeation by an MTZ of 300 μm was much lower than that of 120 μm (Fig. 2b). The same as an MTZ at 120 μm, a higher fluence and spot density further increased hydroquinone permeation with the larger MTZ. Further study examining the permeation of the other permeants was performed using a spot size of 120 μm, pulse fluences of 2 and 4 mJ, and densities of 100 and 400 spots/cm^2. The flux (μg/cm^2/h or nmol/cm^2/h) was measured by the slope of the linear portion of the cumulative amount-time profiles as summarized in Table I. In the case of hydroquinone, the flux of 2-mJ-ablated skin showed 3~4-fold enhancement compared to that of untreated skin. An irradiated fluence of 4 mJ produced further 4~5-fold promotion. As shown in Table I, the enhancement ratio of imiquimod by fractional laser treatment did not surpass the value of hydroquinone. The skin permeation of imiquimod after irradiation was 1~3-times higher than that with no treatment.

Laser-mediated permeation was conducted for the FITC fluorescent dye and its high MW derivatives, FD, at 4~40 kDa. As revealed in Table I, FITC delivery using 400 spots/cm^2 resulted in a 12~13-fold increase, which was superior to that using 100 spots/cm^2 (1~2 fold). Increasing the laser energy did not produce a significant increase ($p>0.05$) in FITC permeation. FD exhibited very low permeation via intact skin. The passive transport of FD20 and FD40 in the receptors was below the detection limit. The fractional CO_2 laser facilitated skin delivery of FD in a more-efficient manner

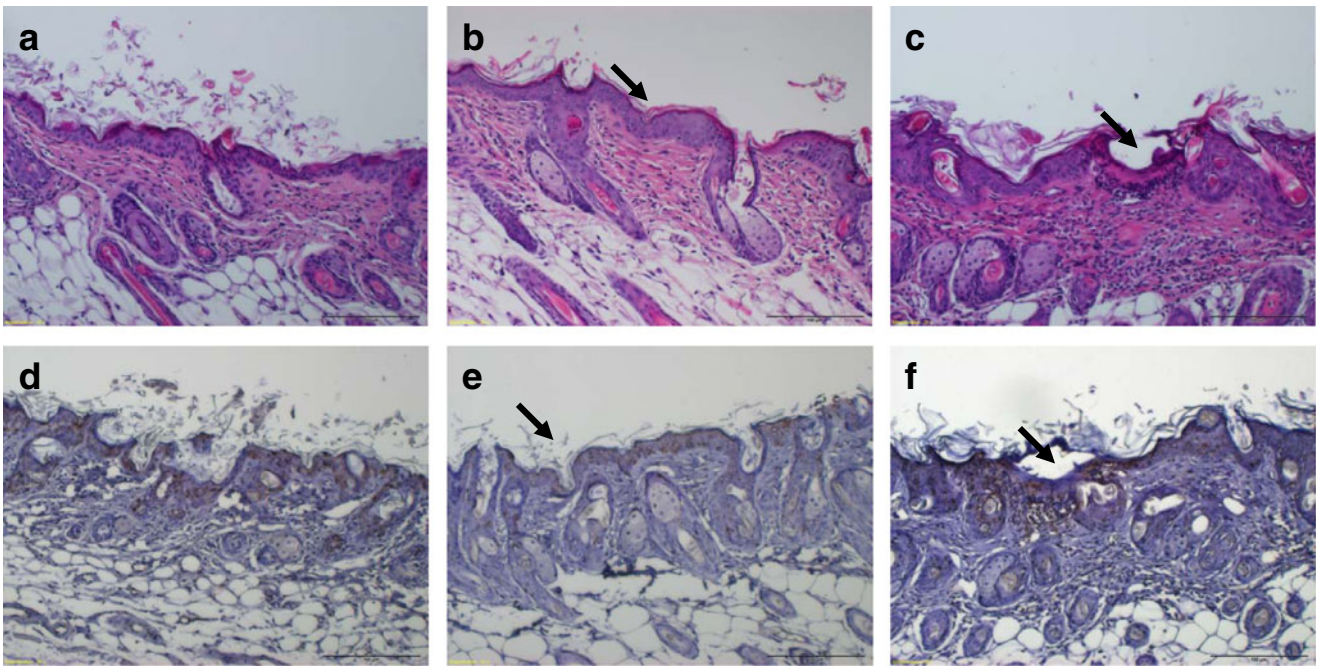

Fig. 1 Hematoxylin and eosin (H&E)-stained histological sections of nude mouse skin without treatment (control) (**a**), skin treated with a fractional laser at 2 mJ and 400 spots/cm^2 (**b**), and 4 mJ and 400 spots/cm^2 (**c**). COX-2-immunostaining histology of nude mouse skin without treatment (control) (**d**), skin treated with a fractional laser at 2 mJ and 400 spots/cm^2 (**e**), and 4 mJ and 400 spots/cm^2 (**f**). The scale represents a length of 100 μm.

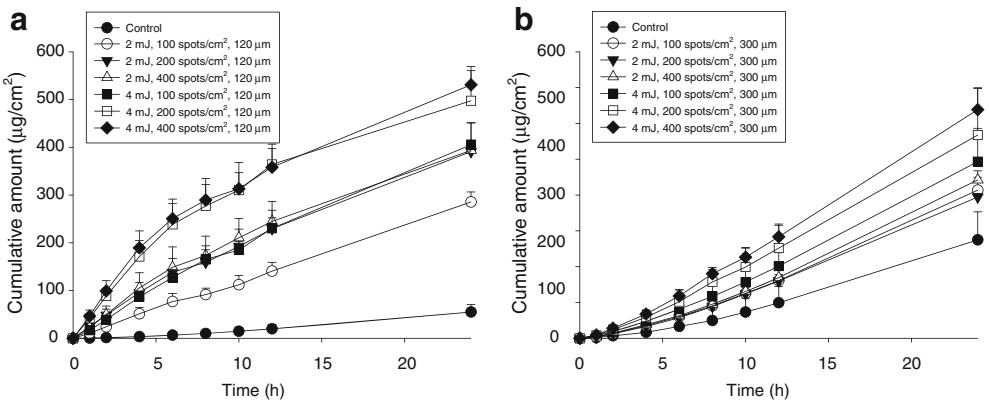

Fig. 2 In vitro cumulative amount-time profiles of hydroquinone by fractional laser treatment of nude mouse skin at spot sizes of 120 (**a**) and 300 μm (**b**) for different fluences and spot densities. Each value represents the mean ± SD (n=4).

than that of the small-molecule permeants. Fluxes of FD4 and FD10 were 86- and 78-fold higher than passive diffusion, respectively, at a fluence of 4 mJ and 400 spots/cm^2. Laser treatment under the same conditions resulted in respective increases in flux levels from 0 to 0.72 and 0.43 nmol/cm^2/h for FD20 and FD40.

Differential Stripping and Cyanoacrylate Skin-Surface Biopsy

The follicular pathway is likely to be a significant route for drug delivery. In order to examine the effect of the laser on the appendageal pathway, the amount of hydroquinone or imiquimod deposited in hair follicles was detected by a combination of stripping and cyanoacrylate casting. Recovery of the drugs from casts is shown in Table II. After a 24-h administration time, 11 μg/ml of hydroquinone was recovered from the follicles of control skin. Increased follicular amounts of hydroquinone from laser-treated skin were not significant (p> 0.05). Significantly more imiquimod was recovered from follicles after laser treatment than in the control group. The imiquimod amount was found to have increased by 13-fold upon laser exposure.

Fluorescence Microscopy

Fluorescence imaging was employed to observe the penetration of FITC, FD20, and QDs into the skin. Figure 3a and b depict images of vertical skin sections with no treatment (blank control) with the same wavelength setups for imaging FITC/FD20 and QDs, respectively. The white lines drawn in Fig. 3a and b are the boundary between the epidermis and dermis. No or negligible fluorescence signals from blank skin at the set wavelength ranges were visualized, indicating a low autofluorescence of the skin itself. In intact skin with FITC application, this small-molecule dye was mainly deposited evenly on the SC surface (Fig. 3c). The yellow circles in the figure show areas of follicles. A very limited movement of this dye to viable skin was observed. There was also widespread accumulation of FITC throughout the SC surface with laser treatment (Fig. 3d). Some fluorescence staining was located in hair follicles, which extended FITC penetration to the dermis. The signal faded from the surface to deeper strata. As shown in Fig. 3e, FD20 predominantly accumulated in follicles with an insignificant signal in the SC and epidermal layers. There was a trend for follicles to express a stronger signal after irradiation compared to the untreated control (Fig. 3f).

Table I The *In Vitro* Flux (μg/cm^2/h for Hydroquinone and Imiquimod, nmol/cm^2/h for FITC and FD) of the Permeants Via Nude Mouse Skin Treated with or Without Fractional CO_2 Laser

Permeant	0 mJ	2 mJ, 100 spots/cm^2	2 mJ, 400 spots/cm^2	4 mJ, 100 spots/cm^2	4 mJ, 400 spots/cm^2
Hydroquinone	4.25 ± 0.75	11.80 ± 0.82 (2.78)	15.84 ± 2.50 (3.73)	16.72 ± 1.86 (3.93)	20.00 ± 1.57 (4.71)
Imiquimod	0.17 ± 0.03	0.23 ± 0.02 (1.35)	0.39 ± 0.03 (2.29)	0.34 ± 0.04 (2.00)	0.49 ± 0.13 (2.88)
FITC	0.69 ± 0.27	1.56 ± 0.97 (2.26)	9.05 ± 1.16 (13.12)	1.10 ± 0.27 (1.59)	8.30 ± 0.74 (12.03)
FD4	0.01 ± 0.002	0.06 ± 0.01 (5.00)	0.56 ± 0.05 (9.33)	0.14 ± 0.02 (11.67)	1.02 ± 0.09 (85.71)
FD10	0.005 ± 0.002	0.15 ± 0.07 (28.04)	0.32 ± 0.05 (57.33)	0.34 ± 0.12 (62.45)	0.43 ± 0.10 (77.62)
FD20	0	0.09 ± 0.02	0.14 ± 0.04	0.15 ± 0.04	0.72 ± 0.07
FD40	0	0.04 ± 0.02	0.07 ± 0.02	0.08 ± 0.02	0.43 ± 0.09

The data behind the mean ± S.D. are the enhancement ratio of the flux of laser-treated group/the flux of untreated group

Each value represents the mean and S.D. (n=4)

Table II The Drug Amount in Hair Follicles (μg/ml) of Nude Mouse Skin Treated After Topical Application with or without Fractional CO_2 Laser

Permeant	0 mJ	4 mJ, 400 spots/cm^2
Hydroquinone	11.02 ± 2.15	12.97 ± 2.20 (1.18)
Imiquimod	0.08 ± 0.02	1.01 ± 0.49 (12.76)

The data behind the mean ± S.D. are the enhancement ratio of the amount of laser-treated group/the amount of untreated group

Each value represents the mean and S.D. (n=4)

QDs as a model nanoparticle were employed to test their ability to penetrate laser-treated skin. In the *in vitro* Franz cell experiment, no QDs were detected in the receptor after 24 h. The skin was subsequently examined by fluorescence microscopy. As shown in Fig. 3g, QD penetration via intact skin was limited to the outermost SC layers with weak intensity. No fluorescence was imaged either in the epidermis or dermis. The imaging of laser-treated skin indicated a clear increase in fluorescence of QDs (Fig. 3h). There was a continuous and homogeneous band of a red signal which extended into the SC. QDs were also detected in the dermis due to deposition in hair follicles (blue circles). The skin regions shown in Fig. 3d, F and H were the areas with MTZs exactly irradiated by the laser, which were like Fig. 1c and f.

In Vivo Skin Permeation

Skin permeation experiments were also conducted *in vivo*. The results were examined using CLSM. Figure 4a and b illustrate images (100×) from intact and laser-irradiated (4 mJ, 400 spots/cm^2) skin with FITC administration for 2 h. The skin was scanned at ~5-μm increments from the skin surface (left to right, top to bottom). The first 6 fragments are sections of the SC and epidermis since the SC and epidermal thicknesses of nude mouse skin are ~10 and ~20 μm, respectively [6]. The green signal in Fig. 4a and b represents the collective emissions of FITC in the tissues. The passive control displayed FITC deposition up to a depth of 25 μm (Fig. 4a). The green fluorescence was distributed in a weak signal according to the summary of 15 total fragments (right panel of Fig. 4a). The skin subjected to laser treatment exhibited fluorescence up to a depth of 75 μm. FITC was distributed in all layers of the skin. The intense fluorescence was derived from follicles and micropores generated by fractional irradiation. As shown in Fig. 4c, a negligible signal was observed for FD20 permeation into intact skin. FD20 entered laser-treated skin through micropores, as evidenced by the green spots throughout the skin. The fluorescence reached a depth of at least 75 μm. CLSM images of the summarized 15 fragments are shown at a higher magnification (630×) in Fig. 5. A greater fluorescence intensity was detected with laser-treated skin than control skin for FITC (Fig. 5a *vs.* b). There was widespread distribution of FITC which was mainly located in follicles, hair shafts, and intercellular regions. The hairs seemed to be intact after laser treatment. A similar result was shown for FD20 (Fig. 5c *vs.* d). FD20 tended to assemble along the edges of corneocytes (Fig. 5d).

Recovery of the Skin Barrier Function

Changes in TEWL were evaluated to survey recovery of the skin barrier function after laser exposure. Figure 6 shows the

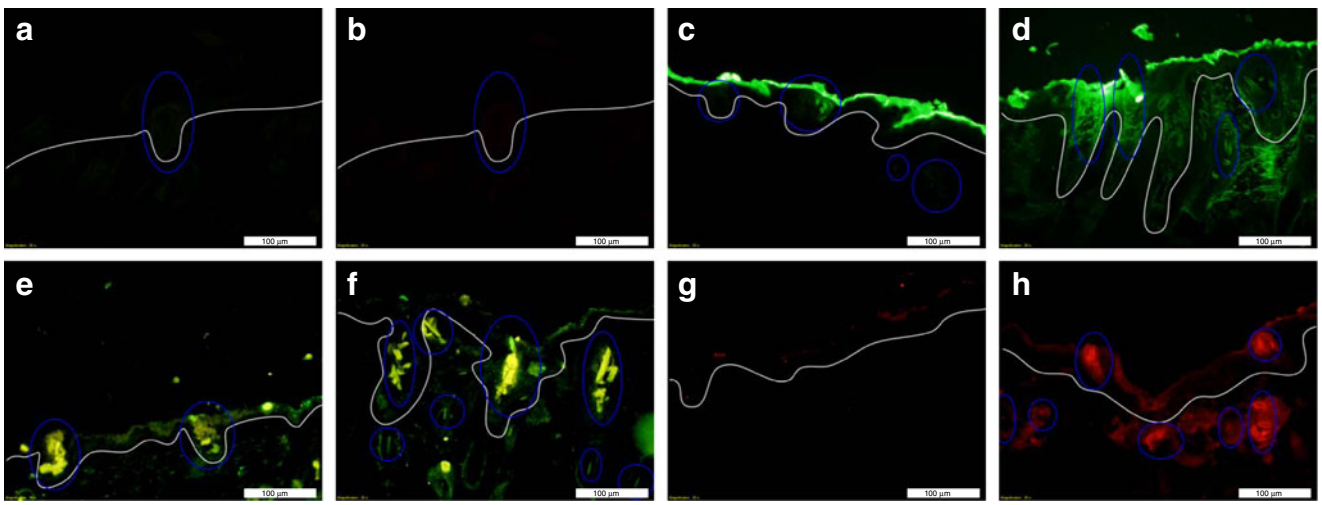

Fig. 3 Fluorescence microscopic images of nude mouse skin: untreated skin detected at 450~490 and 515~565 nm for excitation and emission (**a**); untreated skin detected at 546 and 590 nm for excitation and emission, respectively (**b**); *in vitro* FITC application via untreated skin (**c**); *in vitro* FITC application via laser-treated skin (**d**); *in vitro* FD20 application via untreated skin (**e**); *in vitro* FD20 application via laser-treated skin (**f**); *in vitro* QD application via untreated skin (**g**); *in vitro* QD application via laser-treated skin (**h**). The *white line* is the boundary between epidermis and dermis; the *yellow circle* is the area of hair follicles. The scale represents a length of 100 μm.

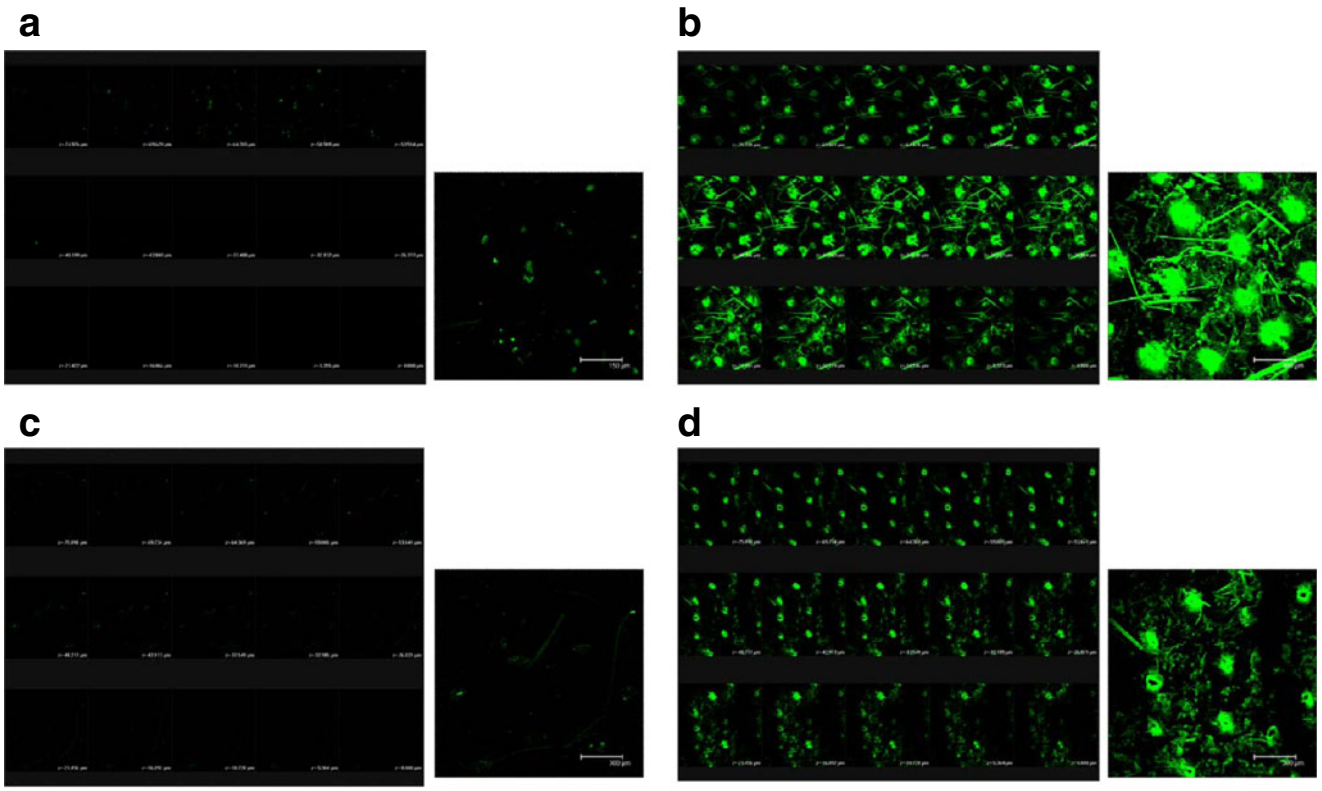

Fig. 4 Confocal micrographs of nude mouse skin with an original magnification of 100x: *in vivo* FITC application via untreated skin for 2 h (**a**); *in vivo* FITC application via laser-treated skin for 2 h (**b**); *in vivo* FD20 application via untreated skin for 2 h (**c**); *in vivo* FD20 application via laser-treated skin for 2 h (**d**). The skin specimen was viewed by confocal microscopy at ~5-μm increments through the Z-axis. A summary of 15 fragments with various skin depths is shown in the right panel of each image. The scale in the summary of 15 fragments represents a length of 300 μm.

Δ values (the value of the treated site minus the value of the untreated site) within 24 h. TEWL immediately increased following fractional laser treatment. A stronger fluence and higher spot numbers resulted in greater augmentation in TEWL. The barrier function returned to a normal level within the detection duration (1 day) under all conditions tested. The barrier function was rapidly repaired to a normal status within the first 12 h after treatment.

DISCUSSION

Laser treatment at 4 mJ resulted in ablation of the SC and some of the epidermis. SC remnants were observed at the treated site. This result was similar to that of a previous study by Chen *et al.* (17). This ensures some integrity of the skin defense for preventing infection and toxin invasion. Compared to 4 mJ, the lower fluence (2 mJ) showed negligible disruption of the skin according to H&E and COX-2 staining. COX-2 plays an essential role in skin pathogenesis such as inflammation and wound healing. The 4-mJ treatment resulted in increased COX-2 expression which may have been due to infiltration of inflammation in the epidermis.

According to the results of skin permeation, the fractional laser at the selected parameter settings could enhance skin transport of all tested permeants. The laser could ablate a part of the SC based on the histopathological observations, leading to a reduced barrier function and increased permeability. In addition to the ablation effect, the laser also disrupted the remnant SC structures by photomechanical waves (2,18). The channels generated by the fractional laser provide a possible pathway to deliver drugs into deeper skin strata, which is like the microneedle technique (19). The fractional laser also increases the surface area for skin permeation. Results of hydroquinone permeation demonstrated a greater enhancement by MTZs of 120~300 μm. Although the larger MTZs ablate larger areas of the SC, the ablated skin depth is consistently reduced compared to a smaller spot size (20). It is because that the total laser energy for MTZs of 120 μm and 300 μm is the same. Since the 300-μm MTZs irradiated more coverage area than 120-μm MTZs, the irradiated depth for 300-μm MTZs was limited to a superficial level. That is, the ablated dimension for different MTZ radii was approximate at a determined fluence. This suggests that the irradiated area is less important in determining drug permeation enhancement. The ablated depth was a predominant factor governing enhancement of

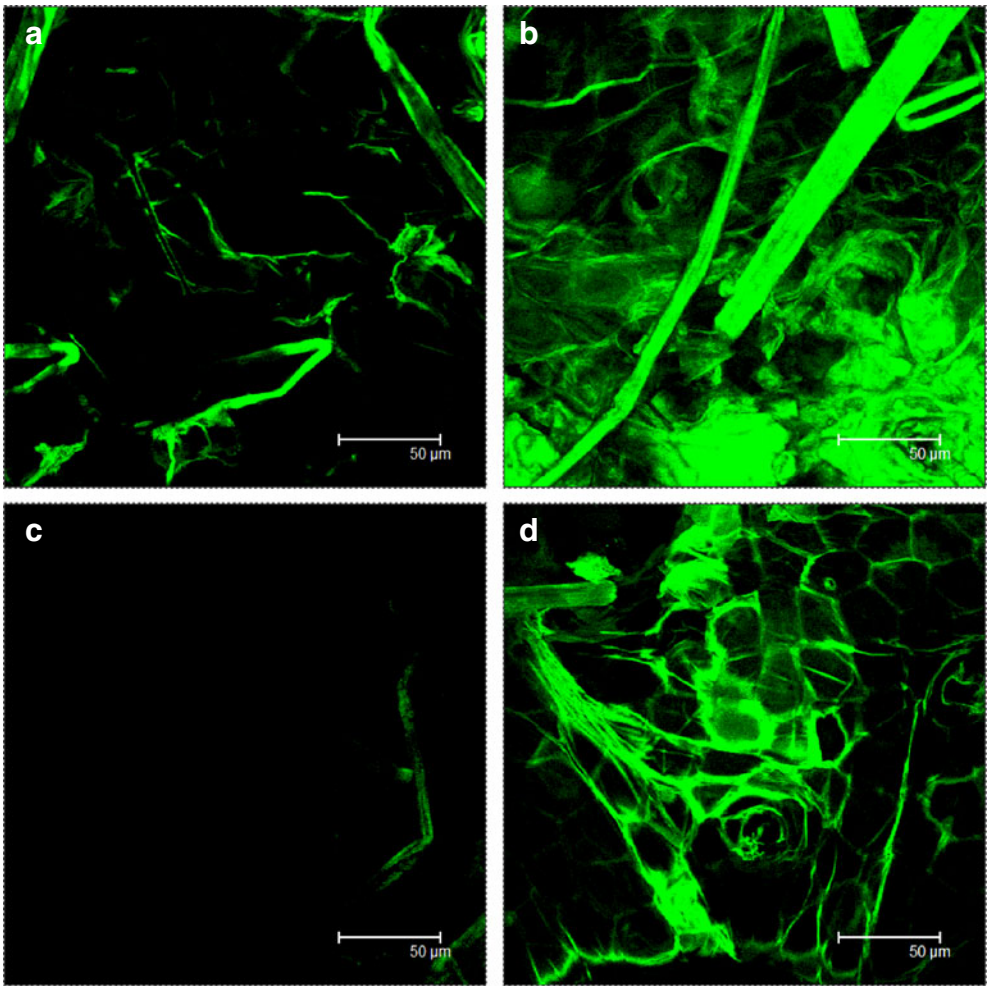

Fig. 5 Confocal micrographs of nude mouse skin at an original magnification of 630×: *in vivo* FITC application via untreated skin for 2 h (**a**); *in vivo* FITC application via laser-treated skin for 2 h (**b**); *in vivo* FD20 application via untreated skin for 2 h (**c**); *in vivo* FD20 application via laser-treated skin for 2 h (**d**). The image is a summary of 15 fragments at various skin depths.

drug transport, such as hydroquinone. The deeper channel could drive the permeant to deeper skin strata for further diffusion into receptor compartment. This suggestion was confirmed by the result that a spot density of 400 spots/cm^2 did not further promote hydroquinone delivery compared to that with 200 spots/cm^2.

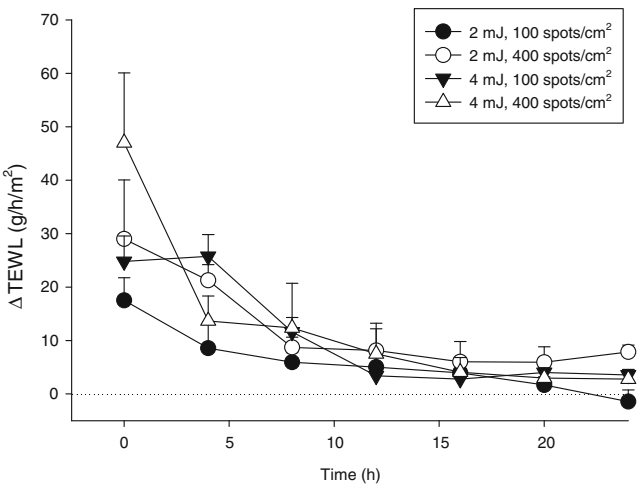

Fig. 6 *In vivo* skin recovery of nude mouse treated with a fractional laser by determining transepidermal water loss (TEWL) during a detection period of 24 h. Each value represents the mean ± SD (n=6).

Macromolecules possess a large size and hydrophilic nature. They penetrate across the SC with difficulty, limiting clinical applications for topical use. To overcome this limitation, the fractional laser was effective in enhancing the skin permeation of FD with MWs ranging 4~40 kDa. FD4 was chosen because of its similarity of molecular size to peptides and nucleotides (21). Some vaccines have a molecular mass which approximates the MW of FD40 (17,22). Some macromolecules easily locate in SC without further diffusion to viable skin because of strong interaction with SC components (23). The partial ablation of the SC layers by laser resulted in the loss of SC interaction to macromolecules, thus dramatically increased their penetration into viable skin and receptor. It was found that the fluence of 4 mJ produced much greater enhancement compared to that of 2 mJ for FD delivery. This may indicate a significant factor of penetration depth in determining macromolecular permeation. A contrary result was observed for small-molecule permeants. The permeation of hydroquinone, imiquimod, and

FITC treated by 4 mJ showed a slightly higher or similar level compared to that treated with the lower fluence. This suggests that superficial ablation was sufficient for small-molecule permeants to penetrate the barrier. It is also possible that a significant removal of the SC can reduce the partitioning of some drugs from the vehicle into the skin, which is an offsetting effect for laser-assisted permeation (14,24).

It is impossible to deliver FD40 through skin in a passive manner, although the deposition in SC is proposed. A previous work (25) demonstrates that FD38, which has a similar MW with FD40, did not penetrate through SC by passive diffusion. The laser increased FD40 permeation from 0 to 0.43 nmol/cm^2/h. This suggests that the fractional laser efficiently delivered macromolecules of at least 40 kDa. Microneedles and thermal ablation are currently used for macromolecular delivery into the skin (26). Nevertheless, microneedle insertion may produce problems involving infection. A previous study (27) also suggests that microneedles generally did not affect follicular structures and the following drug delivery (methyl aminolevulinate) through skin. Thermal ablation may cause a burning sensation and skin structural damage. The fractional laser provides an alternative for delivering macromolecules via the skin. Both hydroquinone and imiquimod induced skin irritation and erythema in some patients (10,28). A shortening of the treatment duration should be considered (29). The laser offers an opportunity to enhance drug absorption, thus reducing the therapeutic period. High inter-individual differences in skin permeation limit topical drug therapy. Another benefit of laser-mediated delivery with precise control is the reduction of inter-subject deviations. After comparing the mean and standard deviation of the flux value, there were relatively small variations in the laser-treated groups. Removal of the SC, which is highly variable among individuals, favors a reduction in the variability (30).

Follicular routes can provide significant access for certain drugs and nanoparticles. Our previous study (24) indicated that a resurfacing laser may affect appendages which could alter drug transport. We systematically explored the role of follicles in skin permeation by laser treatment in this study. Imiquimod had a strong selectivity for hair follicles after irradiation, suggesting the effect of the CO_2 laser on enhancing imiquimod in appendages. Hydroquinone accumulation in follicles was not increased by the laser. This may indicate the lower importance of follicular routes for hydroquinone penetration. With respect to fluorescence microscopy, the broad distribution of passively applied FITC to superficial skin was attributed to easy entrance of small-molecule permeants by intercellular or transcellular routes. The laser did not increase fluorescence in the SC. The offsetting effect of limited partitioning can explain this phenomenon. It was revealed that FITC's distribution was more concentrated along or in the region near hair follicles. This result supports the hypothesis that the fractional laser can enhance follicular delivery of permeants. A similar result was demonstrated for FD20. The main pathway for passively applied FD20 was follicles not intercellular routes because of the large size (6.6 nm) of this macromolecule (31). The laser further increased FD20 permeation into shunt routes. Follicles are generally active in sebum secretion and hair growth. Still 30% of hair follicles are inactive and closed due to the composition of desquamated corneocytes and dry sebum (32). Inactive follicles can be opened by peeling and tape-stripping (16,33), thus increasing permeant penetration into follicles. Nude/hairless mice have follicles of an undeveloped and degenerated nature (34,35), which are like inactive follicles. Laser ablation may open these follicles for effective drug penetration. Since the follicular epithelium exhibits less resistance compared to the interfollicular epithelium (36), opening of follicles by the laser may accelerate drug transport into the skin.

Little is known about QD transport into skin (37). A previous report (38) indicated that QDs of smaller than 10 nm are theoretically able to enter the SC by intercellular pathways. The radius of QDs used in this work was 18 nm, indicating that they might penetrate the SC with difficulty. The surface of QDs was conjugated with a carboxyl group to impart a hydrophilic character. The polar group can strongly bond to hydrated keratin in the SC to retard nanoparticle entrance (39). Ablation by the laser significantly reduced this interaction, facilitating QD influx into deeper strata and follicles. The potential application of nanoparticles for delivering drugs into intact skin is restricted. Follicular routes were suggested to be an important channel for nanoparticle penetration (39,40). Creation of artificial channels and promotion of follicular deposition by a fractional laser may provide a less-invasive technique to introduce nanoparticles into the skin at sufficient depths.

According to the *in vivo* CLSM profiles, laser ablation did not extend FITC's distribution in the skin, but it increased the penetration depth to deeper layers. FITC and FD20 penetrated into laser-irradiated skin along follicles and MTZs. Accumulation of the permeant in the dermis probably involved follicular transport. The permeants radically diffused from microchannels to neighboring tissues. Diameters of green spots for FITC and FD20 were ~200 and ~110 μm, respectively. This was due to the easier diffusion of the small-molecule permeant compared to macromolecules. The distance between the green spots was 450~550 μm, which approximated the established distance of the laser (600 μm). The penetration of the permeants via laser-treated skin seemed to follow intercellular pathways along lipid bilayers. This is reasonable since the laser interacts with SC lipids to disrupt arrays and structures.

For optimization of clinical applicability, the removal of skin layers should be safe to avoid scarring, infection, and toxin entrance. TEWL is representative of damage to the SC barrier (41). The experimental results of TEWL revealed that recovery of the skin barrier function was completed within 12 h after fractional laser exposure. This reepithelialization was much faster compared to that with a conventional CO_2 laser, which required a recovery duration of 4 days (6). As the thermal area of MTZs is small and the surrounding tissue is unaffected by the laser, the lateral migration of intact cells occurs quickly (42). This leads to a faster wound repair process compared to that with a conventional laser.

CONCLUSIONS

Based on the present study, the fractional CO_2 laser offers a promising new strategy to enhance skin transport of drugs, macromolecules, and nanoparticles with reduced disruption of the skin barrier function. Epidermal repair can be completed in a few hours. It was shown that laser exposure was capable of delivering topically applied molecules of a large size, such as FD40 (8.8 nm) and QDs (18 nm). The permeation level can be controlled by modulating the laser fluence or spot numbers. SC ablation and photomechanical waves were the mechanisms enhancing skin permeation. The major pathways for laser-mediated delivery were intercellular and follicular penetration. Follicular transport is a promising route for selective skin diseases such as acne, alopecia, and folliculitis. The fractional laser may be applicable for delivering drugs to treat these disorders. Increased follicular delivery is also beneficial to reach deeper strata and reduce application times. The prospective benefits of fractional laser-assisted permeation are that it can provide a less-invasive method to deliver macromolecules such as proteins, vaccines, and genes compared to a parenteral injection.

ACKNOWLEDGMENTS AND DISCLOSURES

This project was supported by the National Plan for Science and Technology in the Kingdom of Saudi Arabia (grant number: 10-NAN1030-02).

REFERENCES

1. Davidson A, Al-Qallaf B, Das DB. Transdermal drug delivery by coated microneedles: geometry effects on effective skin thickness and drug permeability. Chem Eng Res Des. 2008;86:1196–206.
2. Lee WR, Shen SC, Fang CL, Zhuo RZ, Fang JY. Topical delivery of methotrexate via skin pretreated with physical enhancement techniques: low-fluence erbium:YAG laser and electroporation. Lasers Surg Med. 2008;40:468–76.
3. Gómez C, Costela Á, Garćia-Moreno I, Llanes F, Teijón JM, Blance D. Laser treatments on skin enhancing and controlling transdermal delivery of 5-fluorouracil. Lasers Surg Med. 2008;40:6–12.
4. Pan TL, Wang PW, Lee WR, Fang CL, Chen CC, Huang CM, *et al.* Systematic evaluations of skin damage irradiated by an erbium:YAG laser: histopathologic analysis, proteomic profiles, and cellular response. J Dermatol Sci. 2010;58:8–18.
5. Tsai TH, Jee SH, Chan JY, Lee JN, Lee WR, Dong CY, *et al.* Visualizing laser-skin interaction in vivo by multiphoton microscopy. J Biomed Opt. 2009;14:024034.
6. Lee WR, Shen SC, Wang KH, Hu CH, Fang JY. The Effect of laser treatment on skin to enhance and control transdermal delivery of 5-fluorouracil. J Pharm Sci. 2002;91:1613–26.
7. Haak CS, Illes M, Paasch U, Hædersdal M. Histological evaluation of vertical laser channels from ablative fractional resurfacing: an ex vivo pig skin model. Lasers Med Sci. 2011;26:465–71.
8. Allemann IB, Kaufman J. Fractional photothermolysis – an update. Lasers Med Sci. 2010;25:137–44.
9. Carniol PJ, Harirchian S, Kelly E. Fractional CO_2 laser resurfacing. Facial Plast Surg Clin N Am. 2011;19:247–51.
10. Rendon MI, Gaviria JI. Review of skin-lightening agents. Dermatol Surg. 2005;31:886–9.
11. Metcalf S, Crowson AN, Naylor M, Haque R, Cornelison R. Imiquimod as an antiaging agent. J Am Acad Dermatol. 2007;56:422–5.
12. Kalluri H, Banga AK. Transdermal delivery of proteins. AAPS PharmSciTech. 2011;12:431–41.
13. Chiu TM, Huang CC, Lin TJ, Fang JY, Wu NL, Hung CF. In vitro and in vivo anti-photoaging effects of an isoflavone extract from soybean cake. J Ethnopharmacol. 2009;126:108–13.
14. Lee WR, Shen SC, Al-Suwayeh SA, Yang HH, Yuan CY, Fang JY. Laser-assisted topical drug delivery by using a low-fluence fractional laser: imiquimod and macromolecules. J Control Release. 2011;153:240–8.
15. Hsieh PW, Al-Suwayeh SA, Fang CL, Lin CF, Chen CC, Fang JY. The co-drug of conjugated hydroquinone and azelaic acid to enhance topical skin targeting and decrease penetration through the skin. Eur J Pharm Biopharm. 2012;81:369–78.
16. Teichmann A, Jacobi U, Ossadnik M, Richter H, Koch S, Sterry W, *et al.* Differential stripping: determination of the amount of topically applied substances penetrated into the hair follicles. J Invest Dermatol. 2005;125:264–9.
17. Chen X, Shah D, Kositratna G, Manstein D, Anderson RR, Wu MX. Facilitation of transcutaneous drug delivery and vaccine immunization by a safe laser technology. J Control Release. 2012;159:43–51.
18. Lee S, McAuliffe DJ, Flotte TJ, Kollias N, Doukas AG. Photomechanical transdermal delivery: the effect of laser confinement. Lasers Surg Med. 2001;28:344–7.
19. Donnelly RF, Morrow DIJ, McCarron PA, Woolfson AD, Morrissey A, Juzenas P, *et al.* Microneedle-mediated intradermal delivery of 5-aminolevulinic acid: potential for enhanced topical photodynamic therapy. J Control Release. 2008;129:154–62.
20. Lee WR, Shen SC, Lai HH, Hu CH, Fang JY. Transdermal drug delivery enhanced and controlled by erbium:YAG laser: a comparative study of lipophilic and hydrophilic drugs. J Control Release. 2001;75:155–66.
21. Cao D, Kitamura T, Todo H, Yoo SD, Sugibayashi K. Pretreatment effects of maxibustion on the skin permeation of FITC-dextran. Int J Pharm. 2008;354:117–25.
22. Maeba S, Otake S, Namikoshi J, Shibata Y, Hayakawa M, Abiko Y, *et al.* Transcutaneous immunization with a 40-kDa outer membrane protein of *Porphyromonas gingivalis* induces specific antibodies which inhibit coaggregation by *P. gingivalis*. Vaccine. 2005;23:2513–21.

23. Lanke SSS, Kolli CS, Strom JG, Banga AK. Enhanced transdermal delivery of low molecular weight heparin by barrier perturbation. Int J Pharm. 2009;365:26–33.
24. Lee WR, Shen SC, Pai MH, Yang HH, Yuan CY, Fang JY. Fractional laser as a tool to enhance the skin permeation of 5-aminolevulinic acid with minimal skin disruption: a comparison with conventional erbium:YAG laser. J Control Release. 2010;145:124–33.
25. Lombry C, Dujardin N, Préat V. Transdermal delivery of macromolecules using skin electroporation. Pharm Res. 2000;17:32–7.
26. Prausnitz MR, Langer R. Transdermal drug delivery. Nat Biotechnol. 2008;26:1261–8.
27. Yoo KH, Lee JW, Li K, Kim BJ, Kim MN. Photodynamic therapy with methyl 5-aminolevulinate acid might be ineffective in recalcitrant alopecia totalis regardless of using a microneedle roller to increase skin penetration. Dermatol Surg. 2010;36:618–22.
28. Schön MP, Schön M. Imiquimod: mode of action. Br J Dermatol. 2007;157 Suppl 2:8–13.
29. Swanson N, Abramovits W, Berman B, Kulp J, Rigel DS, Levy S. Imiquimod 2.5% and 3.75% for the treatment of actinic keratoses: results of two placebo-controlled studies of daily application to the face and balding scalp for two 2-week cycles. J Am Acad Dermatol. 2010;62:582–90.
30. Bachhav YG, Heinrich A, Kalia YN. Using laser microporation to improve transdermal delivery of diclofenac: increasing bioavailability and the range of therapeutic applications. Eur J Pharm Biopharm. 2011;78:408–14.
31. Imura Y, Choda N, Matsuzaki K. Magainin 2 in action: distinct modes of membrane permeabilization in living bacterial and mammalian cells. Biophys J. 2008;95:5757–65.
32. Otberg N, Richter H, Schaefer H, Blume-Peytavi U, Sterry W, Lademann J. Variations of hair follicle size and distribution in different body sites. J Invest Dermatol. 2004;122:14–9.
33. Lademann J, Otberg N, Richter H, Weigmann HJ, Lindemann U, Schaefer H, *et al.* Investigation of follicular penetration of topically applied substances. Skin Pharmacol Physiol. 2001;14 Suppl 1:17–22.
34. Fang JY, Lee WR, Shen SC, Wang HY, Fang CL, Hu CH. Transdermal delivery of macromolecules by erbium:YAG laser. J Control Release. 2004;100:75–85.
35. Shim J, Kang HS, Park WS, Han SH, Kim J, Chang IS. Transdermal delivery of minoxidil with block copolymer nanoparticles. J Control Release. 2004;97:477–84.
36. Otberg N, Petzelt A, Rasulev U, Hagemeister T, Linscheid M, Sinkgraven R, *et al.* The role of hair follicles in the percutaneous absorption of caffeine. Br J Clin Pharmacol. 2007;65:488–92.
37. Jeong SH, Kim JH, Yi SM, Lee JP, Kim JH, Sohn KH, *et al.* Assessment of penetration of quantum dots through in vitro and in vivo human skin using the human skin equivalent model and the tape stripping method. Biochem Biophys Res Comm. 2010;394:612–5.
38. Gratieri T, Schaefer UF, Jing L, Gao M, Kostka KH, Lopez RFV, *et al.* Penetration of quantum dot particles through human skin. J Biomed Nanotechnol. 2010;6:586–95.
39. Zhang LW, Monteiro-Riviere NA. Assessment of quantum dot penetration into intact, tape-stripped, abraded and flexed rat skin. Skin Pharmacol Physiol. 2008;21:166–80.
40. Lademann J, Richter H, Teichmann A, Otberg N, Blume-Peytavi U, Luengo J, *et al.* Nanoparticles – an efficient carrier for drug delivery into the hair follicles. Eur J Pharm Biopharm. 2007;66:159–64.
41. Honma Y, Arai I, Sakurai T, Futaki N, Hashimoto Y, Sugimoto M, *et al.* Effects of indomethacin and dexamethasone on mechanical scratching-induced cutaneous barrier disruption in mice. Exp Dermatol. 2006;15:501–8.
42. Goldberg DJ, Berlin AL, Phelps R. Histologic and ultrastructural analysis of melasma after fractional resurfacing. Lasers Surg Med. 2008;40:134–8.